A COMPARATIVE PERFORMANCE ANALYSIS OF FD-NOMA BASED DECENTRALISED V2X SYSTEMS

RAMASONDRANO Andriamanjaka[1], RANDRIAMITANTSOA Paul Auguste[2]

[1] *PhD Student, Telecommunication, Automatic, Signal and Images*
[2] *Professor, Telecommunication, Automatic, Signal and Images*

Doctoral School of Science and Technics of Engineering and Innovation
University of Antananarivo, Madagascar

ABSTRACT

In order to meet the requirements of massively connected devices, different quality of services (QoS), various transmit rates, and ultra-reliable and low latency communications (URLLC) in vehicle-to-everything (V2X) communications, we introduce a full duplex non-orthogonal multiple access (FD-NOMA)-based decentralized V2X system model. We, then, classify the V2X communications into two scenarios and give their exact capacity expressions. To solve the computation complicated problems of the involved exponential integral functions, we give the approximate closed-form expressions with arbitrary small errors. Numerical results indicate the validness of our derivations. Our analysis has that the accuracy of our approximate expressions is controlled by the division of $\frac{\pi}{2}$ *in the urban and crowded scenarios, and the truncation point T in the suburban and remote scenarios. Numerical results manifest that: 1) increasing the number of V2X device, NOMA power, and Rician factor value yields a better capacity performance; 2) effect of FD-NOMA is determined by the FD self-interference and the channel noise; and 3) FD-NOMA has a better latency performance compared with other schemes.*

Keyword: *QoS, V2X, NOMA, FD-NOMA, CAPACITY ANALYSIS*

1. INTRODUCTION

There are two distinct regimes in vehicle to everything (V2X) communications, i.e., the dedicated short-range communications (DSRC) [1], [2] and the cellular-V2X (C-V2X) [3], [4]. DSRC was popular in the past decades. Recently, C-V2X has received much attention with explosively growing devices connecting to the wireless networks. With the help of cellular network, C-V2X can connect more V2X devices [5], [6]; it can establish the link among vehicles, smart infrastructures and pedestrians. C-V2X operates in two modes. First, in the direct communications (DC) mode, V2X devices can directly communicate with each other. Well-known examples include vehicle to vehicle (V2V), vehicle to pedestrian (V2P) communications. Second, in the network-based communications (NC) mode, cellular base station (BS) is playing the dominant role, and the V2X devices communicate with (or with the help of) the cellular, for instance, vehicle to network (V2N), vehicle to infrastructure (V2I) communications. However, the current version of C-V2X (i.e., the long term evolution V2X (LTE-V2X))

cannot fully satisfy the requirements of low latency, various quality of services (QoSs) and different transmit rates [6], [7].

In addition, the existing orthogonal frequency division multiple access (OFDMA)-based LTE-V2X systems need orthogonality. Different from the static or non-mobility wireless communications, moving vehicle caused Doppler effect is a vital problem for OFDMA-based LTE-V2X systems [8]. As is known, carrier frequency offset (CFO) caused by the Doppler effect will lead to inter-carrier interference (ICI) to the OFDM-based wireless communications [9]. In literature, there have been various studies to solve the CFO compensation, see, e.g., [9], [10]. However, because the oscillators can never be oscillating at the identical frequency, in OFDMA-based wireless communications, CFO side-effect always exists even for non-moving circumstance [9].

It is noticed that besides the OFDMA, some fifth generation (5G) technologies can be used to address the issues of low latency [11], various QoS and different transmit rates in V2X communications. From the upper layer perspective, the software-defined networks (SDNs) with its centralized control plan and distributed multiple nodes are more suitable for vehicle communications. With the aid of machine learning and big data analysis, we can monitor all types of events and maintain a global network status [12]. From the physical layer perspective, under the equal frequency resources constraint, NOMA can accommodate more users comparing to the orthogonal multiple access (OMA) scheme. Besides, these users can be with different QoS requirements [13], [14]. In addition, NOMA is insensitive to CFO effect caused by moving vehicles because of its non-orthogonal frequency. NOMA employs the same resource block (RB) for multiple user's transmission, which can alleviate the spectrum bottleneck of wireless communications [15]–[12]. NOMA can pair users with different transmit rates for simultaneous transmission [18]–[20]. On the other hand, while simultaneously transmitting and receiving information, full duplex (FD) can provide faster speed and better spectrum efficiency (SE) performances [13]. Moreover, FD can offer reliable communications [10], which is useful for V2X applications such as navigation and emergency message broadcasting.

1.1 RELATED WORK

Some antecedent works have been done on FD-NOMA. For instance, it was found that FD-NOMA can significantly suppress the co-channel interferences and achieve better performance gains compared to half duplex NOMA (HD-NOMA) and orthogonal multiple access (OMA) [10]. Analysis and simulation results in [14] demonstrated that rate region performance of FD-NOMA outperforms the one with NOMA. Analysis and simulation results in [8] indicates that FD-NOMA improves the 5G's system performance compared to HD-NOMA. Based on the relaying system model, analysis and simulation results in [13] indicated that FD-NOMA outperforms HD-NOMA in terms of outage probability and ergodic sum rate in low signal to noise ratio (SNR) region, but displays an inferior performance in high SNR region.

In V2X communications, there are some existing works on NOMA-V2X and FD-V2X . Based on the NOMA, Khoueiry and Soleymani [5] proposed the graph-based practical encoding and joint belief propagation (BP) decoding techniques, which can achieve any rate pair close to the capacity region. Di et al. [6] employed NOMA for URLLC communications while proposing a NOMA-based mixed centralized/distributed (NOMA-MCD) scheme to reduce the resource collision. In [5], an optimal blind interference alignment scheme was proposed for the coexisting of FD and HD modes. This scheme can improve the sum rate performance in the finite SNR regime. However, most of these studies on NOMA-V2X and FD-V2X communications are based on the NC mode, which is a challenge for connecting massive V2X devices because of the cellular throughput restriction. Although the authors investigated the decentralized NOMA-V2X systems in [25], there has been no capacity analysis for such a system. To the best of our knowledge, a study investigating the impact of FD-NOMA techniques on V2X systems is rare, which motivates us to develop this treatise.

In literature, various channel models are used for the ergodic capacity analysis, for instance, the $\kappa - \mu$ channel model [12], [14] and the $\eta - \mu$ channel model [15]. However, obtaining the closed-form capacity expression in these channel models is difficult because of the involved infinity series operations. Authors thus employed some special conditions and methods to give the closed-form expressions, e.g., μ with positive integer values [8] and the approximate method [7]. On the other hand, the difficulty to obtain a closed-form expression with Rayleigh or Rician channel model lies in the involved exponential integral functions. In order to solve this problem, some approximate methods and algorithms have been proposed, for instance, the Swamee and Ohija method for

exponential integral function [15] and the fast and accurate algorithm for generalized exponential integral function [12]. However, these methods are based on some special conditions (e.g., [12]), or with low accuracies (e.g., [12]). In this paper, we give the approximate closed-form capacity expressions for both Rayleigh and Rician channel models while taming the troublesome exponential integral functions.

In this work, we propose the FD-NOMA-based decentralized V2X system model, and also provide the capacity analysis to obtain the approximate closed-form capacity expressions with high accuracy. We try to answer the following key questions.

- Can we use one solution to meet the requirements of V2X communications? If it is not possible, what about a combination of FD-NOMA techniques?
- If the combination is feasible to satisfy the requirements of V2X communications, what about the capacity and throughput performance of the V2X systems?
- Are there some approximate expressions for the capacity expressions with arbitrary small error and low computational complexity?

The main contributions of this work can be summarized as follows:

- The FD-NOMA-based decentralized V2X systems can partly offload the cellular network.1 Compared to OFDMA, NOMA is insensitive to Doppler effect caused by moving vehicles. In addition, FD-NOMA can accommodate more users with different QoSs and transmit rates for simultaneous transmission and reception.
- Based on the system model, we derive the exact system ergodic capacity expressions and their approximate closed-form expressions for both scenarios. These approximate closed-form expressions are with low computational complexity and controllable arbitrary small errors compared to the existing approximate expressions. Insights from our analysis has 1) the accuracy of our simplified approximate expression in urban and crowded scenario is controlled by the associated division of $\frac{\pi}{2}$

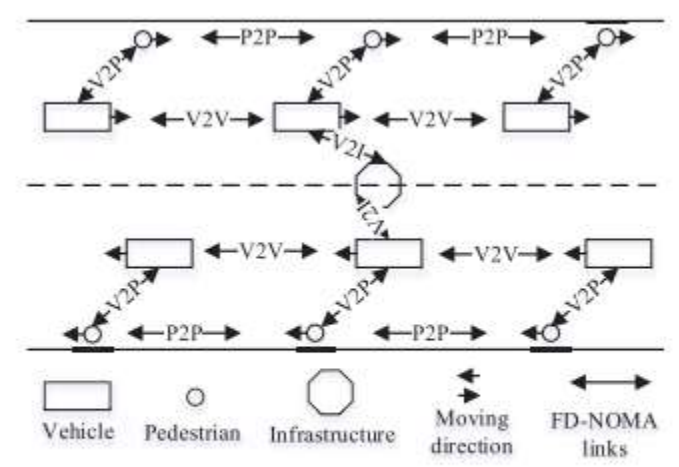

Fig. 1. The $M \leftrightarrow N$ FD-NOMA-based decentralized V2X system model. The communications among V2X devices can be accomplished by FD-NOMA working on the DC mode.

2. SYSTEM MODEL

The FD-NOMA-based decentralized V2X system model is given in Fig. 1. This system is slightly different from the existing ones in the following respects. A) Different from the existing studies on FD-NOMA, no relaying systems are used because of the vehicle's limited energy. B) V2X devices can directly communicate with each other through

DC mode without the cellular's help, and the required contents are obtained from neighboring V2X caches [15]. This system model thus has shorter transmission distance and better latency performance [8]. The cellular network load can be reduced too.

One can notice that to simplify the analysis, only V2V and V2I communications are considered in the existing V2X studies, see, e.g., [11]–[10], [08]–[14]. As discussed, not only the vehicles, V2X aims to connect everything on the road. In order to cope with this trend, in our FD-NOMA-based decentralized V2X systems, all V2X devices (vehicle, pedestrian, traffic lights, etc.) are comprehensively included. The massive connected devices and their various applications are making the V2X communications more complicated. To deal with this intractable problem, in this work, we classify the V2X communications into two scenarios: 1) the urban and crowded scenario and 2) the suburban and remote scenario.

In urban and crowded scenario, Rayleigh fading can be used as the channel model. This is due to the abundant reflection and refraction links between source and destination [13]. In contrast, Rician channel model is suitable for the suburban and remote scenario because of the less obstacles, where we can always establish a dominant light of sight (LoS) path from source to destination [12].

In the FD-NOMA-based decentralized V2X systems, the channel matrix from M sources to N destinations is :

$$H = \begin{bmatrix} h_1 \\ h_2 \\ h_3 \\ \vdots \\ h_N \end{bmatrix} = \begin{bmatrix} h_{1,1} & h_{1,2} & \cdots & h_{1,M} \\ h_{2,1} & h_{2,2} & \cdots & h_{2,M} \\ \vdots & \vdots & \ddots & \vdots \\ h_{N,1} & h_{N,2} & \cdots & h_{N,M} \end{bmatrix} \in \mathbb{C}^{N*M}, \quad (1)$$

where $h_{i,j}$ is the channel between source i and destination j. In this case, the received signal can be given as:

$$y = \mathbf{H}\sqrt{\mathrm{p}} \bullet \mathrm{x} + \mathrm{n}, (9) \quad (2)$$

where $\sqrt{\mathrm{p}} \in \mathbb{C}^{M \times 1}$ is the allocated downlink NOMA power matrix, $\mathrm{x} \in \mathbb{C}^{M \times 1}$ is the downlink transmit signal and $\mathrm{n} \sim \mathcal{CN}(0, \sigma^2 \mathbf{I}_N)$ is the downlink channel noise. Under the condition that $\widehat{\mathbf{H}} = \mathbf{H}^T$ is the uplink channel with FD mode, uplink transmit information with FD mode will be

$$y = \mathbf{H}\sqrt{\mathrm{p}} \bullet \mathrm{z} + \hat{n}, (3)$$

where $\mathrm{z} \in \mathbb{C}^{N \times 1}$ is the uplink information. NOMA power and channel noise vectors thus can be given as $\widehat{\mathbf{p}} = \mathbf{p}^T$, $\widehat{\mathbf{n}} = \mathbf{n}^T$. The total power received by destination n from all M sources is given by $p_n = p_{1,n} + p_{2,n} + \cdots + p_{M,n}$.

Similary,

$$\hat{p}_n = \hat{p}_{n,1} + \hat{p}_{n,2} + \cdots + \hat{p}_{n,M}, \quad (4)$$

$$C_{sum} = \sum_{i=1}^{M} \sum_{j=1}^{N} log_2 \left(1 + \frac{p_{i,j}|h_{i,j}|^2}{\rho\left(\sum_{l=j+1}^{N} p_{i,l} + \eta \hat{p}_{i,k} + \sigma^2\right)}\right), \quad (5)$$

$$C_{sum} = \sum_{i=1}^{M} \sum_{j=1}^{N} log_2 \left[1 + \frac{p\alpha_{i,j}|h_{i,j}|^2}{\rho\left(\sum_{l=j+1}^{N} \alpha_{i,l} + \eta\alpha_{i,k}\right)+1}\right], \quad (6)$$

is the self-interference power when transmitting information to M destinations from source n. *Remark 1:* The received signal is composed of the received downlink information and its self-interference from the FD uplink. (1.10) On the other hand, transmission and reception processes in the FD-NOMA-based decentralized V2X systems are different from the centralized cellular-based communications, i.e., each V2X destination can receive information

with different NOMA power vectors from multiple distributed sources. By invoking the FD-NOMA techniques for simultaneous transmission and reception, the power received and transmitted by each V2X device are p_n, $\hat{p}_n$.

2.1 Ergodic capacity analysis in different scenarios

In the decentralized FD-NOMA V2X systems, transmission channels are uncorrelated. In this case, the considered multiple input multiple output NOMA (MIMO-NOMA) can be treated as a sum of additive single input single output NOMA (SISO-NOMA) links. Moreover, similar to prior works [13], [50], we adopt an increasing order of the channel response, which means $|h_{i,1}|^2 \leq, \ldots, |h_{i,j}|^2 \leq, \ldots, \leq |h_{i,N}|^2, \forall i \in [1, M], j \in [1, N]$, vice versa. In this case, after successive interference cancellation (SIC), NOMA co-channel interference of the i-th user are from the $(i+1)$-th user to the N-th user [12].

According to Shannon theory [10], shown at the top of this page, see the equation in the top of next page. Here $\sum_{l=i+1}^{N} p_{i,l}$ yields the co-channel interference from neighboring users after SIC, $\eta\hat{p}_{i,k}$ is the self-interference by FD uplink, σ2 is the channel noise power, respectively. Additionally, η is the coefficient of self-interference with $\eta \in [0, 1]$, which makes our expressions versatile to describe different schemes. For instance, in FD-NOMA scheme, large value of η denotes the strong FD self-interference, and small value denotes the weak FD self-interference. On condition that $\eta = 0$, the expression reduces to the pure NOMA expression. On the basis, normalizing the channel noise power value will give , shown at the top of this page. Here ρ is the SNR, and we use $\alpha_{i,j}, \alpha_{i,l}, \alpha_{i,k}$ to denote the allocated NOMA power coefficient with FD transmission in line with a normalized channel noise power value. In the sequel, we adopt the normalized noise power.

We first analyze the achievable sum capacity in urban and crowded scenario. Note that we use the superscript a and c to distinguish different scenarios. In urban and crowded scenario, PDF of instantaneous signal to interference plus noise ratio (SINR) in each time slot, say, $\gamma_{i,j}$, is given by

$$f^a(\gamma_{i,j}) = \frac{1}{\bar{\gamma}_{i,j}} e^{-\frac{\gamma_{i,j}}{\bar{\gamma}_{i,j}}}, \quad (7)$$

where

$$\bar{\gamma}_{i,j} = \frac{\rho\alpha_{i,j}}{\rho\left(\sum_{l=i+1}^{N} \alpha_{i,l} + \eta\alpha_{i,k}\right) + 1}$$

is the averaged channel power gain of each destination. As is well known, ergodic capacity is achieved by experiencing all the channel fading states, which means

$$C_{i,j}^{a} = \mathbb{E}\left[\log_2(1+\gamma_{i,j})\right] \quad (8)$$

$$= \int_0^{+\infty} \log_2(1+\gamma_{i,j}) f^a(\gamma_{i,j}) d\gamma_{i,j}$$

$$= \int_0^{+\infty} \log_2(1+\gamma_{i,j}) \frac{1}{\bar{\gamma}_{i,j}} e^{-\frac{\gamma_{i,j}}{\bar{\gamma}_{i,j}}} d\gamma_{i,j}.$$

in the following theorem, we provide the exact ergodic capacity expression of the FD-NOMA-based decentralized V2X systems.

In urban and crowded scenario, the exact achievable sum ergodic capacity of the FD-NOMA-based decentralized V2X systems is:

$$C_{sum}^{a} = \sum_{i=1}^{M}\sum_{j=1}^{N} e^{\frac{1}{\bar{\gamma}_{i,j}}} E_1\left[\frac{1}{\bar{\gamma}_{i,j}}\right] \log_2 e \ , \quad (9)$$

where $E_1(x)$ is the exponential integral function that defined as

$$E_1(x) = \int_x^{\infty} \frac{e^{-t}}{t} dt. \quad (10)$$

In order to verify the tightness of this expression, we compare the performances of the exact expression, the approximate expression and the well-known Swamee and Ohija approximation. Note that the Swamee and Ohija approximation expression is given by [8]

$$E_1(x) = (A^{-7.7} + B)^{-0.13} \ ,$$

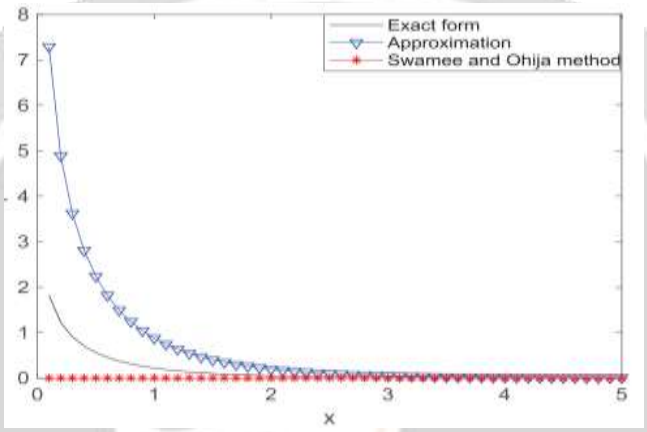

Fig -2 : Comparison of the exact, approximation and Swamee and Ohija-based expressions

Additionally, one can see from Fig. 2 that the approximation curve displays a similar curvature to the exact curve. We can expect that a coefficient factor to the closed-form expression might improve the accuracy, i.e.,

$$E_1'(x) = q4\pi \sum_{k=1}^{n+1}\sum_{s=1}^{t+1} a_k \sqrt{b_k} a_s e^{-b_k b_s x} \ . \quad (11)$$

Consequently, our task is to find out a q satisfying

$$|E_1'(x) - E_1(x)| \leq \epsilon.$$

Here we use $\epsilon = 0.00001$. After some manipulations, we notice that when $q = \frac{1}{4}$, the above condition is met (e.g., $|E_1'(1) - E_1(1)| = |0.2193827 - 0.2193839| = 1.2187 \times 10^{-6}$). We thus have an approximate closed-form expression

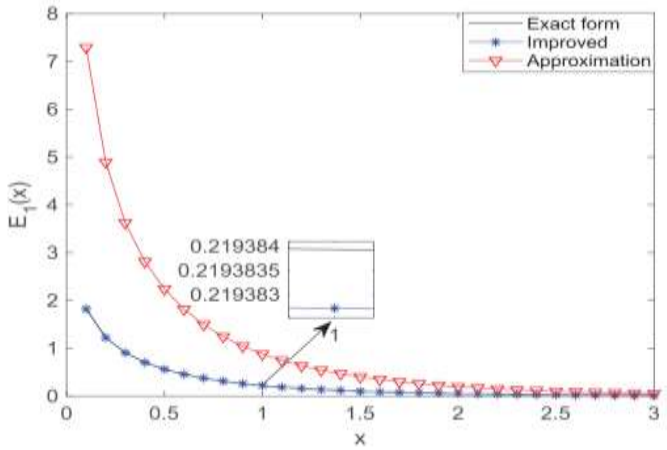

Fig -3 : Comparison of the exact, improved and approximate expressions

Of $E_1(1)$ as

$$E_1(x) \approx \pi \sum_{k=1}^{n+1} \sum_{s=1}^{t+1} a_k \sqrt{b_k} a_s e^{-b_k b_s x} \quad (12)$$

2.2 Ergodic Capacity Analysis in Suburban and Remote Scenario

In the subsection III. A, we have obtained both exact and approximate forms of the capacity of the FD-NOMA-based decentralized V2X systems in urban and crowded scenario. In this subsection, we focus on the system capacity analysis in the suburban and remote scenario. We use K as the Rician factor (which is the ratio between the deterministic and random fast-fading component). It is noticed that in Rician channel, we have

$$K = \frac{r^2}{2\omega^2}. \quad (13)$$

where r^2 yields the channel gain of LoS component, $2\omega^2$ is the average channel power gain of all NLoS components. By defining the total average power gain as $\bar{\gamma}$ and following the prior work in [12], PDF of $\gamma_{i,j}$ can be given as :

$$f^c(\gamma_{i,j}) = \frac{K+1}{\bar{\gamma}_{i,j}} e^{\left[-K - \frac{(K+1)\gamma_{i,j}}{\bar{\gamma}_{i,j}}\right]} I_0\left(2\sqrt{\frac{K(K+1)\gamma_{i,j}}{\bar{\gamma}_{i,j}}}\right). \quad (14)$$

Here $I_0(\cdot)$ is the first kind modified Bessel function with zeroth order. By following a similar procedure of the previous analysis, we can obtain Theorem 2.

Theorem 2: Exact ergodic capacity expression of the FD-NOMA-based decentralized V2X systems in suburban and remote scenario is given by

$$C_{sum}^c = \sum_{i=1}^{M} \sum_{j=1}^{N} \frac{e^{-K}}{\ln 2} e^{\frac{K+1}{\bar{\gamma}_{i,j}}} \sum_{m=0}^{\infty} \frac{K^m}{m!} \sum_{l=1}^{m+1} E_{m-l+2}\left(\frac{K+1}{\bar{\gamma}_{i,j}}\right).$$

Here $E_n(x)$ is the generalized exponential integral function defined as [15]

$$E_n(x) = \int_1^{\infty} \frac{e^{-xt}}{t^n} dt \ (\mathrm{Re}(x) > 0), \quad (15)$$

where $\mathrm{Re}(x)$ yields the real part of x.

This expression is still intractable to use directly because of the involved infinite factorial and generalized exponential integral expressions. In order to tame this troublesome problem, we give one approximate expression with arbitrary small error by invoking the truncation method in the sequel. We find that the following expression

$$\sum_{m=0}^{\infty} \frac{K^m}{m!} \sum_{q=1}^{m+1} E_{m-q+2}\left(\frac{K+1}{\bar{\gamma}_{i,j}}\right). \quad (16)$$

has an upper ceiling approximation, as shown by **Corollary 2**. In this case, th ıpacity can be given by an approximate expression with much lower computation complexity and arbitrary small error, ϵ.

Corollary 2: By truncating the infinite series with regard to T , the capacity expression is approximately given as

$$C_{sum}^{c} = \sum_{i=1}^{M}\sum_{j=1}^{N} \frac{e^{-K}}{\ln 2} e^{\frac{K+1}{\bar{\gamma}_{i,j}}} \sum_{m=0}^{T} \frac{K^m}{m!} \sum_{q=1}^{m+1} E_{m-q+2}\left(\frac{K+1}{\bar{\gamma}_{i,j}}\right), \quad (17)$$

The truncation error is

$$\sum_{i=1}^{M}\sum_{j=1}^{N} \frac{e^{-K}}{\ln 2} e^{\frac{K+1}{\bar{\gamma}_{i,j}}} \sum_{m=T+1}^{\infty} \frac{K^m}{m!} \sum_{q=1}^{m+1} E_{m-q+2}\left(\frac{K+1}{\bar{\gamma}_{i,j}}\right), \quad (18)$$

Remark 3: One can notice that the accuracy of the approximate expression is controlled her words, we may obtain an approximate expression with an arbitrary small error when

$$\sum_{i=1}^{M}\sum_{j=1}^{N} \frac{e^{-K}}{\ln 2} e^{\frac{K+1}{\bar{\gamma}_{i,j}}} \sum_{m=T+1}^{\infty} \frac{K^m}{m!} \sum_{q=1}^{m+1} E_{m-q+2}\left(\frac{K+1}{\bar{\gamma}_{i,j}}\right) < \epsilon.$$

Table 1 - Consumed time (Second) of APP and MC simulations with ρ = 15 DB

Urban and crowded scenario	App	0,0002	0,0001	0,0001	0,0001	0,0004	0,0000	0,0000	0,0000
	MC	83,0272	89,2913	83,0986	80,8462	81,7240	87,6330	91,5975	87,3378
Suburban and remote scenario	App	0,0781	0,0153	0,0036	0,0034	0,0066	0,0035	0,4032	0,06056
	MC	92,9720	89,8830	89,6005	92,4459	95,3015	97,2475	95,9309	94,8763

Insight from **Corollary 2** has that the system capacity expression is determined by $M, N, \bar{\gamma}_{i,j}$ and K. With M, N increasing, the system capacity always increases. The precise effects of $\gamma^{-}i, j$, K to the capacity are still nonintuitive, which will be discussed in the following section.

3. NUMERICAL RESULTS

In this section, we perform the Monte Carlo simulations to verify the validity of our analysis. We also perform simulations to exposit the effects of different parameters to the system capacity, and compare the performance between FD-NOMA and NOMA schemes based on the decentralized FD-NOMA-enabled V2X systems. Due to variable parameters, we separately explain them and their values in the following simulations.

In these simulations, for the sake of compactness, one source with multiple destinations are used, where the source employs the FD-NOMA scheme to serve these destinations. We also assume that the allocated NOMA power variance is growing linearly with a normalized noise variance value (e.g., with 4 users, the NOMA power vector is $a_i = [4, 3, 2, 1]$), where $a_i = [\alpha_{i,1}, \ldots, \alpha_{i,N}]$). Additionally, $\eta = 0.1, \alpha_{i,k} = 5$ are used. As clearly shown by Fig. 4 and Fig. 5, our analytical results3 and the MC results almost exactly coincide, which demonstrates the

validity of our analysis. For instance, in Fig. 4, with $\rho = 15\,dB, 1 \leftrightarrow 4$, the Mont Carlo and approximative results are respectively 3.6865, 3.6866 Bit/S/Hz.

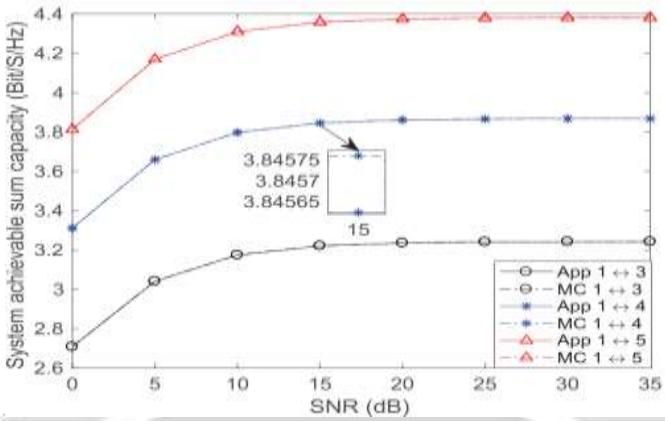

Fig -4 : Comparison of the system achievable sum capacity performances with approximative and Mont Carlo results in suburban and remote scenario. The analytical results are obrained according to (31)

Under the same condition, as shown in Fig. 5, Mont Carlo result and approximative result are 3.8458, 3.8455 Bit/S/Hz, respectively. The differences are less than 0.001 Bit/S/Hz in both scenarios. We also observe that as the values of N, ρ increases, the system capacity always increases. By comparing Fig. 4 and Fig. 5, we notice that under the same condition, capacities in suburban and remote scenario always outperform the ones in urban and crowded scenario (for instance, in $1 \leftrightarrow 3$ case, $\mathrm{SNR} = 0\,\mathrm{dB}$, $C_{sum}^{c} = 125\% C_{sum}^{a}$; $\mathrm{SNR} = 30\mathrm{dB}, C_{sum}^{c} = 103\% C_{sum}^{a}$). This is because of the less propagation loss with a dominant LoS path between source and destination in the suburban and remote scenario.

In order to verify the benefits of our analytical expressions, we compare the consumed time of App and MC simulations in Table I with $\rho = 15\,dB$ as an example. In these simulations, eight-core 3.4 GHz processors, 16 GB memory and windows 10 64-bit operating system are used. The results are rounded off to four decimal places. As shown in Table I, the consumed time of our analytical expressions are about 10^6 times shorter than the MC simulations.

In the next step, we check the effect of Rician factor K to the system capacity in suburban and remote scenario. In order to keep K as the only variable, we do some manipulations as follows: 1) we keep all variables consistent except K; 2) with normalized noise power value and 3 destinations, we set $a_i = [1, 2, 3]$. The simulation results of the system capacity vs the K value in suburban and remote scenario is given in Fig. 5.

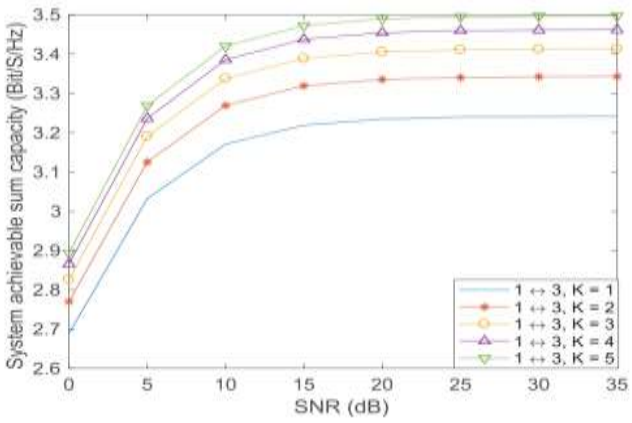

Fig -5 : Comparison of the capacities with different K values

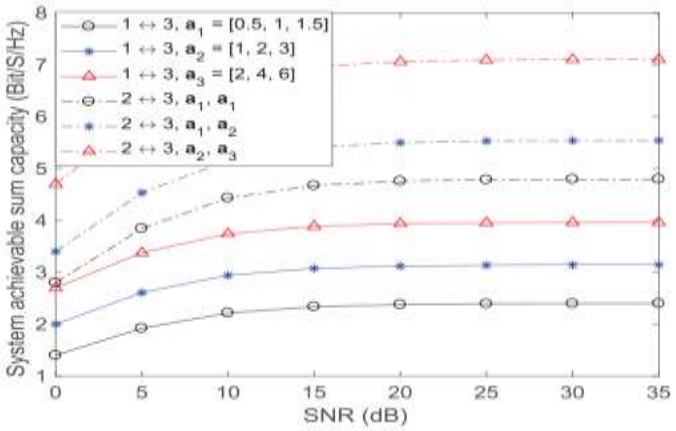

Fig -6 : Comparison of the capacities with different power values and source numbers

We notice that as the K increases, system capacity also increases. This is because the higher K brings in a stronger LoS component and a weaker multi-path propagation loss.

Besides the effects of N, ρ, K, the effects of M and ai to the system capacity are also checked with: 1) a linearly growing power value with $M = 1\,(i.e., a_1 = [0.5, 1, 1.5], a_2 = [1, 2, 3], a_3 = [2, 4, 6])$; 2) different NOMA power vectors with $M = 2\,(i.e., 2 \leftrightarrow 3, a_1, a_3$ denote that two sources are transmitting information to 3 destinations with FD-NOMA, where the NOMA power vector are a_1, a_2, respectively). The simulation results are given by Fig. 7 and Fig. 8. As shown by the solid lines in both figures, increasing the power values leads to better capacity performance, which is due to the increased SNR value. For instance, in 1 ↔ 3 case and SNR = 20 dB, we have $C_{sum}^{a}(a_2) = 131\% C_{sum}^{a}(a_1)$. We can also confirm from both figures that as M increases, the system capacities also increase.

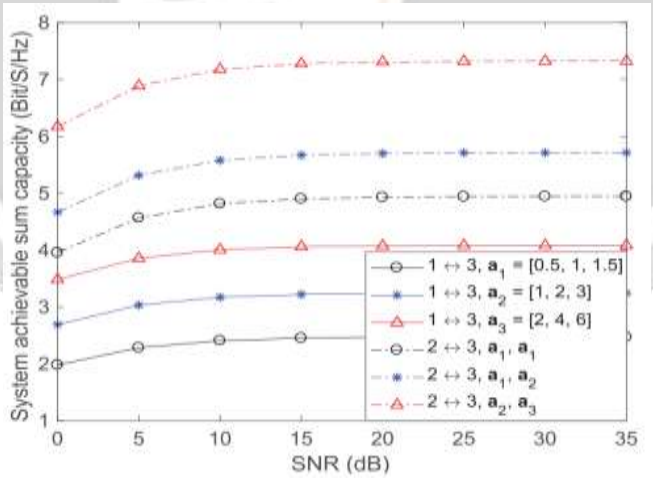

Fig -7 : Comparison of the capacities with different power values and source numbers

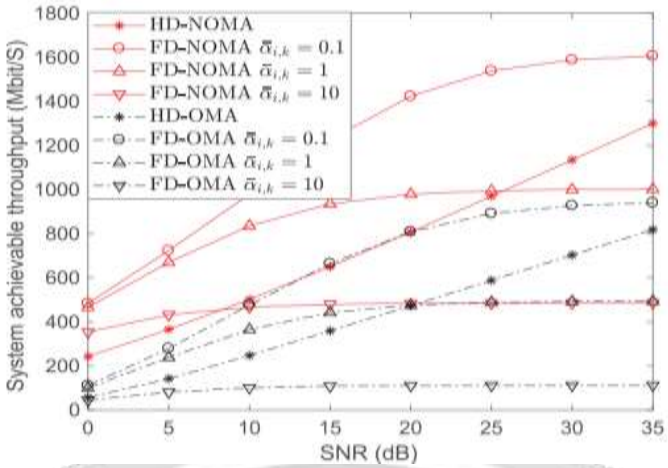

Fig -8 : System achievable throughput comparisons with FD-NOMA, NOMA, FD-OMA and HD-OMA schemes in urban and crowded scenario

Finally, we compare the achievable throughputs with FD-NOMA, NOMA, FD-OMA and HD-OMA schemes in different scenarios. The results are given in Fig. 9 and Fig. 10. In these simulations, carrier bandwidth B = 100 MHz, $a_i = [3, 2, 1], \eta = 0.1$ and $\alpha_{i,k} = 0.1, 1, 10$ are used. In order to be fair, we average the allocated power in FD-OMA and HD-OMA schemes. As shown in both figures, NOMA scheme has a better throughput performance compared to OMA scheme. Moreover, with a smaller value of $\alpha_{i,k}$, FD-NOMA always outperforms the other schemes (HD-NOMA, FD-OMA, HD-OMA). However, the benefit of FD-NOMA decreases while $\alpha_{i,k}$ increasing. This is mainly due to the increased FD self-interferences. We also notice that even with a higher FD self-interference value, FD-NOMA outperforms NOMA in low SNR scenario (i.e., $\rho \in [0, 5]\ dB$).

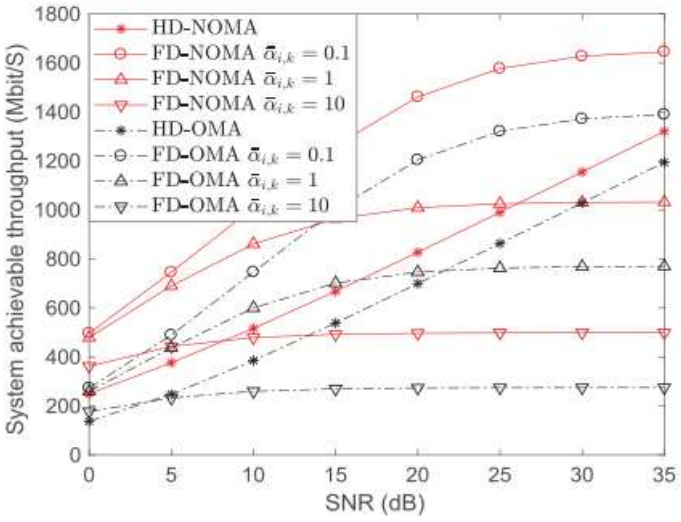

Fig -9 : System achievable throughput comparisons with FD-NOMA, NOMA, FD-OMA and HD-OMA schemes in suburban and remote scenario

This is because in low SNR scenario, channel noise is the dominant factor compared to FD self-interference. In contrast, FD-NOMA self-interference becomes the dominant factor in high SNR scenario, NOMA scheme without FD self-interference thus has a better throughput performance. It is also worth noting that the effective transmission time is limited because of the fast moving V2X devices. FD-NOMA enabled bidirectional transmission can greatly reduce the transmission latency compared to other schemes. For example, compared to HD-NOMA and HD-OMA, FD-NOMA only needs a half latency time to transmit the same amount of data by its simultaneous transmission and reception scheme.

4. CONCLUSIONS

In conclusion, we proposed the FD-NOMA-based decentralized V2X systems. We classified the V2X communications into two typical scenarios, i.e., the urban and crowd scenario and the suburban and remote scenario, and then derived the exact system capacity expressions in both scenarios. To tackle down the capacity expression's intractable calculations in both scenarios, we further obtained their simplified approximate expressions. Insights of our analysis are that the accuracy of our simplified approximate expression in urban and crowded scenario is determined by the associated division of $\frac{\pi}{2}$ (with respect to exponential integral function $(E_1(x))$, and the accuracy of simplified approximate expression in suburban and remote scenario is determined by the truncation point T (with respect to generalized exponential integral function $(E_n(x))$. Numerical results demonstrate the validity and effectiveness of our analytical results. Compared to MC method, the consumed time is greatly reduced by our Approximation expressions. Simulation results also demonstrated that the system capacity performance can be enhanced by increasing the number of V2X devices, NOMA power and Rician factor (suburban and remote scenario), and the effectiveness of FD-NOMA is determined by the FD self-interference and the channel noise. In addition, FD-NOMA can greatly reduce the system latency compared to other schemes.

5. REFERENCES

[1]. N. Bhushan, Junyi Li, D. Malladi, R. Gilmore, D. Brenner, A Damnjanovic, R. Sukhavasi, C. Patel, and S. Geirhofer. Network densification: the dominant theme for wireless evolution into 5g. IEEE Communications Magazine, February 2014

[2]. S. Singh, H. S. Dhillon, and J. G. Andrews, «*Offloading in heterogeneousnetworks: modeling, analysis and design insights,* » IEEE Trans. On Wireless Commun., vol. 12, no. 5, pp. 2484 – 2497, May 2013.

[3]. T. Bai and R. W. Heath Jr., «*Coverage and rate analysis for millimeter wave cellular networks,* » IEEE Trans. Wireless Commun., vol. 14, no. 2, pp. 1100–1114, Feb. 2015

[4]. T. Bai, R. Vaze, and R. Heath, «*Analysis of blockage effects on urban cellular networks,* »IEEE Trans. Wireless Commun., vol. 13, no. 9, pp.5070–5083, Sept. 2014